

# IntrinsicNGP: Intrinsic Coordinate based Hash Encoding for Human NeRF

Bo Peng Jun Hu Jingtao Zhou Xuan Gao Juyong Zhang\*

University of Science and Technology of China

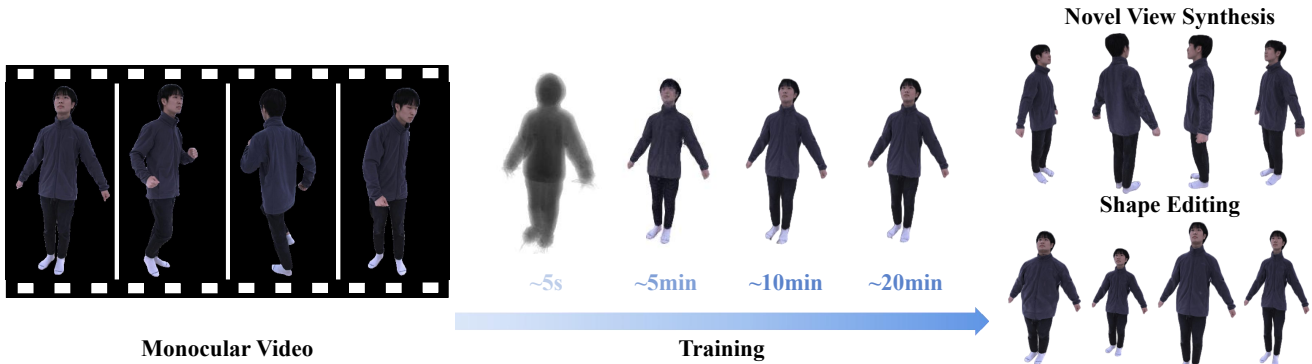


Figure 1. For a 400-frame monocular video with a resolution of  $1224 \times 1024$ , IntrinsicNGP can train from scratch and converge within few minutes on a single RTX 3090 and supports novel view synthesis as well as human shape editing.

## Abstract

Recently, many works have been proposed to utilize the neural radiance field for novel view synthesis of human performers. However, most of these methods require hours of training, making them difficult for practical use. To address this challenging problem, we propose IntrinsicNGP, which can train from scratch and achieve high-fidelity results in few minutes with videos of a human performer. To achieve this target, we introduce a continuous and optimizable intrinsic coordinate rather than the original explicit Euclidean coordinate in the hash encoding module of instant-NGP. With this novel intrinsic coordinate, IntrinsicNGP can aggregate inter-frame information for dynamic objects with the help of proxy geometry shapes. Moreover, the results trained with the given rough geometry shapes can be further refined with an optimizable offset field based on the intrinsic coordinate. Extensive experimental results on several datasets demonstrate the effectiveness and efficiency of IntrinsicNGP. We also illustrate our approach's ability to edit the shape of reconstructed subjects.

## 1. Introduction

Novel view synthesis of human performance is a significant research problem in computer vision and computer graphics. It has wide applications in many areas, such as

sports event broadcasts, video conferences, and VR/AR. Although this problem has been widely studied for a long time, existing methods still require quite a long computation time. This shortcoming causes the technology not to be easily used by public users. Therefore, a high-fidelity novel view synthesis of human performance training within few minutes will have significant value for practical use.

Traditional novel view synthesis methods need dense inputs for 2D image-based methods [8] or require depth cameras for high-fidelity 3D reconstruction [7] to render realistic results. Some model-based methods [2, 4, 13] could reconstruct explicit 3D mesh from sparse RGB videos but lack geometry detail and tend to be unrealistic. Recently, several works have applied NeRF [18] to synthesize novel view images of dynamic human bodies. NeuralBody [22], AnimatableNeRF [21], HumanNeRF [31], and other works [14, 15, 26, 34, 36] are able to synthesize high-quality rendering images and extract rough body geometry from sparse-view videos of the human body by combining human body priors with the NeRF model. However, most of these works require quite a long time to train for each subject, which is caused by the expensive computation cost of NeRF. Recently, with the well-designed multi-resolution hash encoding [20], the training speed of NeRF has been improved by several orders. However, the current strategy of INGP is based on extrinsic coordinate and only works for static scenes, and how to extend it to dynamic scenes has not yet been explored.

In this paper, we propose IntrinsicNGP, a novel view synthesis method for the human body, which can synthesize high-fidelity novel view results of human performance even with a monocular camera and can converge within few minutes. These characteristics make IntrinsicNGP practical for ordinary users. We achieve these targets via a novel intrinsic coordinate representation based on the estimated rough geometry shape, which can extend multi-resolution hash encoding to dynamic objects while aggregating information across frames. Unlike most previous works [21, 31], which represent dynamic human bodies as a deformation field and an implicit field in the canonical space, we propose an intrinsic coordinate representation independent of human motion and directly learn a radiance field based on it. The basic idea is illustrated in Fig. 2.

Specifically, given human performers’ videos from sparse views, we recover the rough human surface for each frame with existing reconstruction methods like VideoAvatar [2] and EasyMocap [1]. For a query point in the current frame’s space, we project it onto the current frame’s human surface to get its corresponding nearest point on the surface. The nearest point and corresponding signed distance value are used to represent the query point since they roughly remain unchanged among human motion.

Although simply applying the 3D coordinate of the corresponding point on the template surface of the nearest point and the signed distance value as the intrinsic coordinate would suffice for our needs, this representation is not easy to be further optimized. This is because the template surface is intrinsically a 2D manifold. Thus it is difficult to directly optimize the 3D coordinate of the corresponding point such that the optimized point is still on the surface. To address this problem, we parameterize the human surfaces to a continuous 2D plane. In practice, we use the UV coordinate of the nearest point and the signed distance value as our intrinsic coordinate. We denote the mapping from query points to intrinsic coordinates as UV-D mapping and call the mapped range UV-D grid. The UV-D grid records color and density information of the space around the geometry proxies like the UV map records texture information of its corresponding 2D manifold surface. Moreover, since our UV-D grid is a continuous and connected domain, we optimize an offset field within this space to model detailed non-rigid deformations. With our proposed intrinsic coordinate as the input of multiresolution hash encoding rather than the original Euclidean coordinate, we can thus construct the neural radiance field for human performance based on INGP [20]. Additionally, since IntrinsicNGP represents the human body as an explicit surface and implicit radiance field based on it, we can render the reconstructed subject with modified body shapes by editing the input geometry proxy.

In summary, the contributions of this paper include the following aspects:

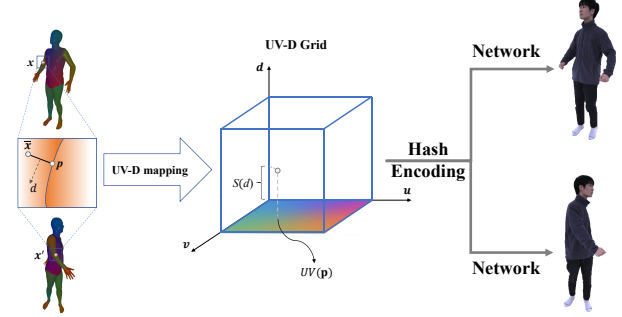


Figure 2. **Basic Idea of IntrinsicNGP.** The corresponding points at different frames are mapped to the same intrinsic coordinate in the UV-D grid, and thus get the same density and color via hash encoding and NeRF network.

- We propose an intrinsic coordinate representation for hash encoding based INGP, which can aggregate inter-frame information and thus extend the scope of INGP’s application from static scenes to dynamic scenes.
- With the help of estimated human body surface, we can reconstruct the neural radiance field of a dynamic human in few minutes, and thus achieve high-fidelity novel view and novel shape synthesis of human performance with a monocular camera.

## 2. Related Work

**Neural Radiance Field based Human Reconstruction**  
 NeRF(neural radiance field) [18] represents a static scene as a learnable 5D function and adopts volume rendering to render the image from any given view direction. Recently, some researchers have focused on applying the neural radiance field to human reconstruction. Neuralbody [22] utilizes a set of latent codes anchored to a deformable mesh which is shared at different frames. H-NeRF [34] employs a structured implicit human body model to reconstruct the temporal motion of humans. AnimatableNeRF [21] introduces deformation fields based on neural blend weight fields to generate observation-to-canonical correspondences. Surface-Aligned NeRF [35] defines the neural scene representation on the mesh surface points and signed distances from the surface of a human body mesh. Neural Actor [15] integrates texture map features to refine volume rendering. HumanNeRF [36] employs an aggregated pixel-alignment feature and a pose embedded non-rigid deformation field for tackling dynamic motions. A-NeRF [26] proposes skeleton embedding serves as a common reference that links constraints across time. Neural Human Performer [14] introduces a temporal transformer and a multi-view transformer to aggregate corresponding features across space and time. Weng et al. [31] optimize for NeRF representation of the person in a canonical T-pose and a motion field that maps the estimated canonical representation

to every frame of the video via backward warps, making it only requires monocular inputs. Although these methods can generate high-fidelity novel view synthesis results for human performer, they are costly to train and evaluate.

**Acceleration of Neural Radiance Field Training** Although NeRF [18] could generate high-fidelity novel view synthesis, its long training time cannot be accepted in practical use. Therefore, how to improve the training speed of NeRF has been widely studied since its emergence of NeRF. DS-NeRF [6] utilizes the depth information supplied by 3D point clouds to speed up convergence and synthesize better results from fewer training views. KiloNeRF [23] adopts thousands of tiny MLPs instead of one large MLP, which could achieve real-time rendering and train 2~3x faster. Plenoxels [25] represent a scene as a sparse 3D grid with spherical harmonics and thus can be optimized without any neural components. DVGO [27] adopts a representation consisting of a density voxel grid and a feature voxel grid with a network for view-dependent appearance. DIVeR [32] utilizes a similar scene representation but applies deterministic rather than stochastic estimates during volume rendering. Recently, INGP [20] proposed to store the features of the voxel grid in a multi-resolution hash table and employ a spatial hash function to query the features, thus can significantly reduce the number of optimizable parameters. These methods are only applicable to static scenes, how to apply them to dynamic objects is still a problem.

**Human Shape Reconstruction from Images** Some traditional model-based works only require the single view RGB input. SMPLify [4] utilizes SMPL [17] model to represent human bodies and obtain per-frame parameters via optimization. SMPL+D based method Videoavatars [2] first calculates per-frame poses using the SMPL model, then optimizes for the subject’s shape in the canonical T-pose. Kolotouros et al. [13] adopt GraphCNN to directly regress the 3D location of the SMPL template mesh vertices, relaxing the heavy reliance on the model’s parameter space. Though these methods cannot achieve photo-realistic view synthesis due to the limitation of the explicit parametric model, their fast-generated human surface can introduce human priors for implicit methods.

Instead of optimizing parameters per scene, some works utilize networks to learn the priors of humans from ground truth data. PIFu [24] concatenates pixel’s aligned feature and depth of a given query point as the input of an MLP to obtain a 3D human occupancy field. StereoPIFu [9] introduces the volume alignment feature and relative z-offset when giving a pair of stereo videos, which can effectively alleviate the depth ambiguity and restore absolute scale information. BCNet [11] proposes a layered garment representation that can support more garment categories and re-

cover more accurate geometry.

To capture better geometry surfaces of humans, representing the human body as the zero isosurfaces of a SDF(signed distance field) has become popular. PHORHUM [3] modifies the geometric representation to SDF to get finer geometry and normal, so they can simultaneously estimate detailed 3D geometry and the unshaded surface color together with the scene illumination. ICON [33] infers a 3D clothed human meshes from a color image by utilizing a body-guided normal prediction model and a local-feature-based implicit 3D representation conditioned on SMPL(-X). SelfRecon [10] represents the human body as a template mesh and SDF in canonical space and utilizes a deformation field consisting of rigid forward LBS deformation and small non-rigid deformation to generate correspondences. Given monocular self-rotation RGB inputs, these methods are capable of generating meshes of clothed humans.

### 3. Method

Given a captured video of a human performer, we aim to train from scratch and generate a free-viewpoint video of the performer in few minutes. We first recover the rough human surfaces  $\{\mathbf{T}_t \mid t = 0, \dots, N_t - 1\}$  and the body masks  $\{\mathbf{M}_t \mid t = 0, \dots, N_t - 1\}$  for each frame via EasyMocap [1] and MiVOS [5], where  $t$  is the index of frame and  $N_t$  is the total number of frames.

Fig. 3 shows the overview of IntrinsicNGP. We first provide some background in Sec3.1. We present intrinsic coordinate representation in Sec3.2, which can aggregate inter-frame information and extend hash encoding to dynamic human cases. Hash encoding and neural radiance field based on intrinsic coordinate are introduced in sec3.3. Finally, our training strategy and loss are presented in sec3.4.

#### 3.1. Background

**Neural Radiance Field** A neural radiance field (NeRF) [18] represents a static 3D scene as an MLP function  $F_\omega$  that outputs the radiance emitted in each direction  $\mathbf{v}$  at each point  $\mathbf{x}$  in space, and a density at each point. Then a volume rendering strategy is used to render the neural radiance field for any given camera pose. In practice, for any query point  $\mathbf{x}$  and view direction  $\mathbf{v}$ , NeRF encodes them with a positional encoding that projects a coordinate vector into a high-dimensional space. These high dimensional vectors are then fed into  $F_\omega$  to predict density  $\sigma(\mathbf{x})$  and radiance  $\mathbf{c}(\mathbf{x}, \mathbf{v})$  at input point  $\mathbf{x}$ . While rendering, NeRF samples one ray  $\gamma = \mathbf{o} + \mathbf{u}\mathbf{v}$  per pixel and then calculates the pixel’s color by the following volume rendering strategy [16]:

$$\mathbf{C}(\gamma) = \sum_{i=1}^N \alpha(\mathbf{x}_i) \prod_{j < i} (1 - \alpha(\mathbf{x}_j)) \mathbf{c}(\mathbf{x}_i), \quad (1)$$

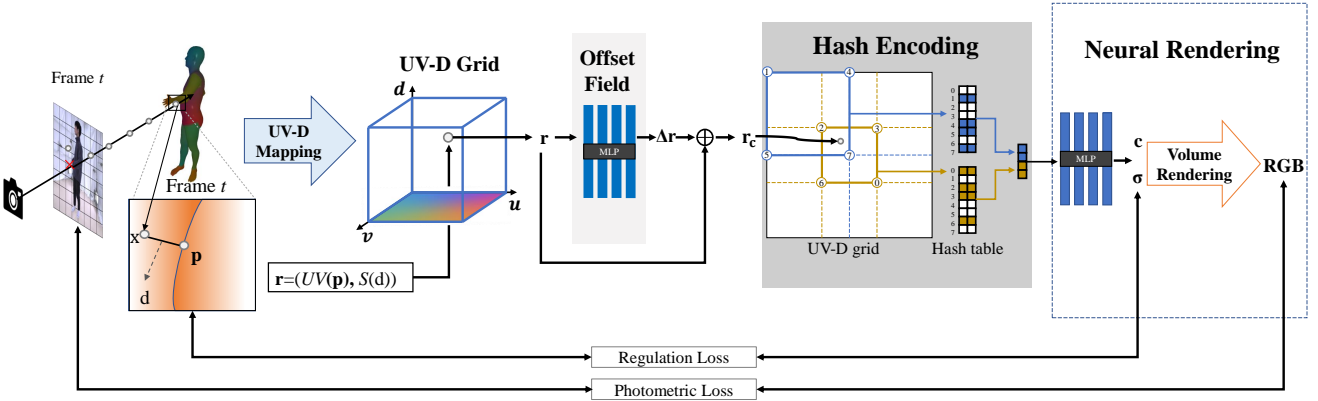


Figure 3. **Overview of IntrinsicNGP.** Given a sample point  $\mathbf{x}$  at frame  $t$ , we obtain its intrinsic coordinate  $\mathbf{r}$  conditioned on current human surfaces to aggregate the corresponding point information of different frames. An offset field is proposed to optimize the intrinsic coordinate to model detailed non-rigid deformation. Then we utilize multi-resolution hash encoding to get the high dimensional feature, which is the encoded input to the NeRF MLP to regress color and density of  $\mathbf{x}$ .

where  $\alpha(\mathbf{x}_i) = 1 - \exp(-\sigma(\mathbf{x}_i)\delta_i)$ ,  $\mathbf{x}_i = \mathbf{o} + t_i\mathbf{v}$  are sample points on the ray, and  $\delta_i = u_{i+1} - u_i$  are the distance between adjacent sample points.

**Multi-resolution Hash Encoding** To increase the training speed, we adopt the multi-level hash encoding in INGP [20]. Specifically, INGP maintains  $L$  levels hash tables, and each table contains  $J$  feature vectors with dimensionality  $F$ . We denote the feature vectors in the hash tables as  $\mathcal{H} = \{\mathcal{H}_l \mid l \in \{1, \dots, L\}\}$ . Each table is independent, and stores feature vectors at the vertices of a grid with resolution  $N_l$ , which is chosen evenly between the coarsest and finest resolution  $N_{\min}, N_{\max}$ . We set  $N_{\min} = 16$ , and  $N_{\max}$  is the same as the original resolution of the input videos.

We denote the multi-resolution hash encoding with learnable feature vectors  $\mathcal{H}$  as  $\mathbf{h}(\cdot|\mathcal{H})$ . For a specific level  $l$ , a 3d-vector  $\mathbf{z} \in \mathbf{R}^3$  is scaled by that level's resolution and then spans a voxel by rounding up and down  $[\mathbf{z}_l] := [\mathbf{z} \cdot N_l], [\mathbf{z}_l] := [\mathbf{z} \cdot N_l]$ . The feature of  $\mathbf{z}$  is tri-linear interpolated by the feature vectors at each corner of the voxel. The feature vectors at each corner are queried from  $\mathcal{H}_l$  using the following spatial hash function [30]:

$$\text{hash}(\mathbf{r}) = \left( \bigoplus_{i=1}^3 r_i \pi_i \right) \bmod \mathbf{T}, \quad (2)$$

where  $\bigoplus$  denotes the XOR operation and  $\pi_i$  are unique, large prime numbers. The feature vectors of  $\mathbf{z}$  at  $L$  levels are then concatenated to produce  $\mathbf{h}(\mathbf{z}|\mathcal{H}) \in \mathbf{R}^{LF}$ .

### 3.2. Intrinsic Coordinate Representation

Given a sample point  $\mathbf{x}$  at frame  $t$ , we expect to construct an intrinsic coordinate representation conditioned on

the current surface shape. This representation aims to ensure that the corresponding points in different frames will be mapped to the same intrinsic coordinate and thus get the same feature vectors in hash encoding. Specifically, given two points  $\mathbf{x}$  and  $\mathbf{x}'$  at different frame  $t$  and  $t'$  respectively, we should have  $\text{Map}(\mathbf{x}|\mathbf{T}_t) = \text{Map}(\mathbf{x}'|\mathbf{T}_{t'})$  if they are in correspondence. We observe that when the human body moves over time, the nearest point of the query point on the human surface and the corresponding signed distance value are roughly unchanged. Based on this observation, we utilize the nearest point  $\mathbf{p}$  on the current human surface  $\mathbf{T}_t$  and corresponding signed distance  $d$  to represent the query point  $\mathbf{x}$  at frame  $t$ . We then give two different intrinsic coordinate representations based on  $\mathbf{p}$  and  $d$  in the following.

**XYZ-D Representation** We first adopt the coordinate of the corresponding point  $\bar{\mathbf{p}}$  of  $\mathbf{p}$  on the template surface  $\mathbf{T}_0$  and signed distance value  $d$  as intrinsic coordinate, which we denote as XYZ-D representation. Formally, given any point  $\mathbf{x}$  at frame  $t$ , we calculate its intrinsic coordinate as:

$$\text{XYZD}(\mathbf{x}|\mathbf{T}_t) = (\text{Coord}(\bar{\mathbf{p}}), S(d)), \quad (3)$$

where  $\text{Coord}(\cdot)$  represents the normalized 3D coordinate,  $S(\cdot)$  means a sigmoid function, which is used to normalize  $d$  to  $[0, 1]$ .

**UV-D Representation** Although XYZ-D representation can aggregate information across frames, it is difficult to be optimized.

The XYZ of the XYZ-D representation refers to points on the template surface  $\mathbf{T}_0$ . Thus, the feasible region of this optimization problem should be  $\mathbf{T}_0 \times \mathbb{R}$ , which is not

convex in  $\mathbb{R}^4$ . Therefore, optimizing in  $\mathbb{R}^4$  without additional constraints will optimize outside the feasible region, leading to a meaningless result.

To solve this problem, we map the human surface sequence to the same smooth region in 2D space since the human surface is intrinsically a 2D manifold. In practice, we utilize the UV coordinate  $UV(\mathbf{p}|\mathbf{T}_t)$  of  $\mathbf{p}$  and corresponding signed distance value  $d$  as the intrinsic coordinate of  $\mathbf{x}$ , which we denote as UV-D representation. Formally, we define our UV-D mapping as follows:

$$UV\mathcal{D}(\mathbf{x}|\mathbf{T}_t) = (UV(\mathbf{p}|\mathbf{T}_t), S(d)), \quad (4)$$

where  $\mathbf{p}$  and  $d$  means the nearest point on  $\mathbf{T}_t$  and the corresponding signed distance value,  $UV(\cdot|\mathbf{T}_t)$  refers to UV mapping from  $\mathbf{T}_t$  to a pre-calculated UV map.  $UV\mathcal{D}(\cdot|\mathbf{T}_t)$  maps points around  $\mathbf{T}_t$  to  $[0, 1]^3$ , and we denote it as UV-D grid. Just like UV texture map records texture information of its corresponding 2D manifold, the UV-D grid records color and density information of the points around the geometry proxies.

**Offset Field** The recovered human surfaces are not always accurate enough and can not model details, which limits the mapping accuracy of our intrinsic coordinate, as shown in Fig. 4. To recover details, we utilize an offset field:

$$\Delta\mathbf{r} = F_\phi(\mathbf{r}, \mathbf{e}_t), \quad (5)$$

where  $\mathbf{r}$  is an intrinsic coordinate,  $F_\phi$  refers to an MLP with learnable weight  $\phi$ ,  $\mathbf{e}_t$  means conditional variable at frame  $t$ . We also adopt the hash encoding scheme to  $F_\phi$  to speed up training.

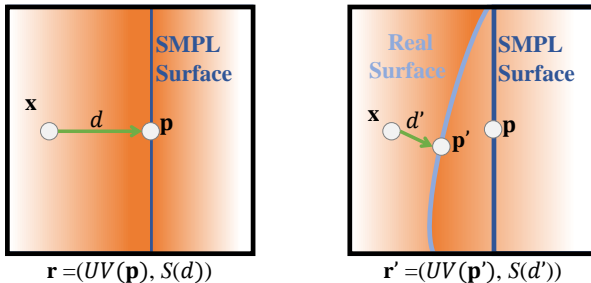


Figure 4. **Purpose of the offset field.** The rough geometry of SMPL surface result in a biased intrinsic coordinate  $\mathbf{r}$ , so we utilize an offset field to optimize it.

### 3.3. Intrinsic NGP

Although INGP [20] is able to converge in a short time, it only works for static scenes. To extend this fast training strategy to dynamic objects, we apply multi-resolution hash encoding based on our intrinsic coordinate instead of the original explicit Euclidean coordinate. The encoded input is

then fed into NeRF MLP  $F_\omega$  to regress radiance and density. The radiance field in the UV-D grid is defined as:

$$(\sigma(\mathbf{r}), \mathbf{c}(\mathbf{r})) = F_\omega(\mathbf{h}(\mathbf{r}|\mathcal{H})), \quad (6)$$

where  $\sigma(\mathbf{r})$  and  $\mathbf{c}(\mathbf{r})$  are the density and radiance of a point  $\mathbf{r}$  in the UV-D grid,  $F_\omega$  represents the MLP function with learnable weights  $\omega$ .

The density and radiance of a query point  $\mathbf{x}$  at frame  $t$  can now be defined as:

$$(\sigma_t(\mathbf{x}), \mathbf{c}_t(\mathbf{x})) = (\sigma(\mathbf{r} + \Delta\mathbf{r}), \mathbf{c}(\mathbf{r} + \Delta\mathbf{r})), \quad (7)$$

$$(\sigma_t(\mathbf{x}), \mathbf{c}_t(\mathbf{x})) = F_\omega(\mathbf{h}(\mathbf{r} + \Delta\mathbf{r}|\mathcal{H})), \quad (8)$$

where  $\mathbf{r} + \Delta\mathbf{r}$  is the optimized intrinsic coordinate of  $\mathbf{x}$ . Finally, the color of each sample ray is calculated with Eq. (1).

### 3.4. Training

We use the following loss function to jointly optimize  $\omega, \phi, \mathcal{H}$

#### 3.4.1 Photometric Loss

We minimize the render error of all observed images, and the loss function is defined as:

$$L_{\text{rgb}} = \sum_{\gamma \in \mathcal{R}} \left\| \tilde{\mathbf{C}}(\gamma) - \mathbf{C}(\gamma) \right\|_2, \quad (9)$$

where  $\mathcal{R}$  is the set of rays passing through image pixels and  $\tilde{\mathbf{C}}(\gamma)$  is the ground truth color.

#### 3.4.2 Regulation Loss

**Mask Loss** We require the weight sum of the ray to match the input masks.

$$L_{\text{mask}} = \sum_{\gamma \in \mathcal{R}} (\mathbf{W}(\gamma)(1 - \mathbf{M}(\gamma)) + (1 - \mathbf{W}(\gamma))\mathbf{M}(\gamma)), \quad (10)$$

where  $\mathbf{W}(\gamma) = \sum_{i=1}^N \alpha(\mathbf{x}_i) \prod_{j < i} (1 - \alpha(\mathbf{x}_j))$  is the weight sum of the ray  $\gamma$ ,  $\mathbf{M}(\gamma) = 1$  if  $\gamma$  is sampled from the pixel in the masked area otherwise 0.

**Distance Loss** If a point is far from the human body, its density should be close to 0. Therefore, we use an exponential function to penalize density outside the human body.

$$L_{\text{dist}} = \sum_{\mathbf{x} \in \mathcal{X}} \sigma(\mathbf{x}) \exp(\varphi(d(\mathbf{x}))\beta), \quad (11)$$

where  $\mathcal{X}$  is the set of points sampled on the rays in  $\mathcal{R}$ ,  $\beta$  is a hyper parameter and  $\varphi(\cdot)$  refers to the Relu function.



Figure 5. Qualitative comparison result on ZJU-MoCap dataset and our custom data.

**Offset Regularization Loss** The output of the offset field should be relatively small. Thus we apply the following:

$$L_{\text{dfm}} = \sum_{\mathbf{x} \in \mathcal{X}} \|F_\phi(UVD(\mathbf{x}|\mathbf{T}_t), \mathbf{e}_t)\|_2. \quad (12)$$

### 3.4.3 Training Strategy

The total loss function is formulated as:

$$L_{\text{total}} = L_{\text{rgb}} + \lambda L_{\text{reg}}. \quad (13)$$

Where  $L_{\text{reg}}$  is the weighted combination of the losses defined in Sec 3.4.2. We set  $\lambda = 1$  for the first 400 iterations to learn a coarse geometry of the human body, and then set  $\lambda = 0.1$  to learn the details mainly through inverse rendering.

### 3.5. Implementation Details

We implement our code on top of the torch-`ngp`<sup>1</sup> codebase [19, 20, 28, 29]. We optimize with Adam [12] using a learning rate decay from  $2 \cdot 10^{-3}$  to  $2 \cdot 10^{-5}$ . To speed up evaluation, we render a wide mask of the human performer with SMPL meshes and only apply volume rendering in the masked area. For a  $1080 \times 1080$  monocular video of 200 frames, we need around 3K iterations to converge (about 12 minutes on a single NVIDIA GeForce GTX3090 GPU).

## 4. Experiments

To demonstrate the effectiveness of our method, we conduct comparison experiments on monocular videos. Some ablation studies are also discussed to evaluate the necessity of our modules. For more experiments and results, please

<sup>1</sup><https://github.com/ashawkey/torch-ngp>

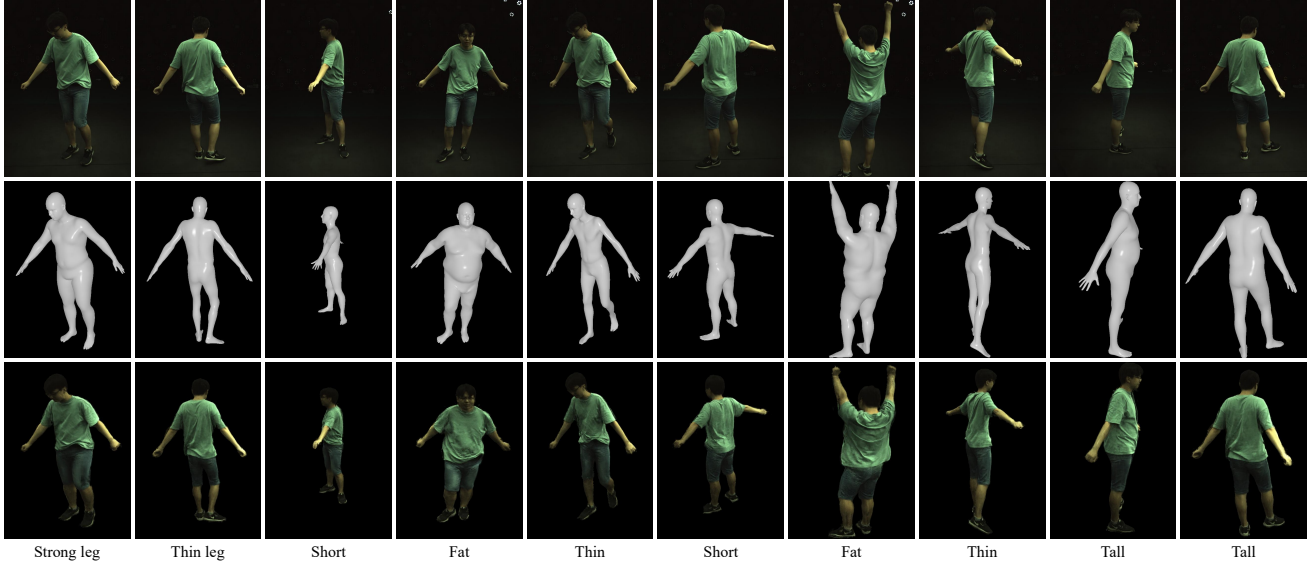


Figure 6. **Application of Shape editing.** The reconstructed model by our method can be used for shape editing. Top to bottom: reference video input, target shape, and output result.

see our supplementary material and video.

#### 4.1. Dataset

To evaluate our method’s reconstruction ability from single-view input, we capture some custom data, which includes monocular videos of human performers and the corresponding SMPL meshes. Each video contains the whole body information of the performer from a single view. Videos from other views are provided for evaluation. We also employ ZJU-Mocap [22] dataset for comparison with state-of-the-art methods.

**metrics** Consistent with NeRF [18], we use two standard metrics to quantify novel view synthesis results: peak signal-to-noise ratio (PSNR) and structural similarity index (SSIM). Following NeuralBody [22], we only calculate these metrics on pixels inside the 2D bounding box, which is obtained per view from the input masks.

#### 4.2. Comparison

We compare with state-of-the-art implicit human novel view synthesis methods:

1) AnimatableNeRF [21] uses deformation fields based on neural blend weight to aggregate per-frame information to reconstruct neural radiance field in canonical space.

2) NeuralBody [22] reconstructs per frame’s neural radiance field conditioned at body-structured latent codes, which are diffused to the whole space via SparseConvNet.

3) SelfRecon [10] reconstructs the clothed human body by combining implicit and explicit representations to recover coherent space-time geometries.

4) HumanNeRF [31] decomposes human motion as a skeletal motion and a pose-based non-rigid motion and then reconstructs the canonical space’s neural radiance field.

We perform this experiment on ZJU-Mocap [22] and our custom data. Specifically, we choose 5 objects (313, 377, 386, 392, 394) from ZJU-Mocap and 3 objects from our custom data with relatively high image quality and use “Camera (1)” for training and other views for evaluation.

We use the official open-source code of these methods to compare with our method. We disabled HumanNeRF’s Pose correction module since this would cause misalignment with the ground truth image in novel view, leading to relatively low PSNR and SSIM scores.

As shown in Fig. 5, SelfRecon, HumanNeRF and our method can produce satisfactory results similar to the ground truth even on completely unobserved views, while NeuralBody and AnimatableNeRF tend to produce results with blurs and color differences. Tab. 1 shows the quantitative results for training frames and novel poses respectively. Our method outperforms NeuralBody and AnimatableNeRF for all objects and under all metrics. HumanNeRF and SelfRecon outperform us by a small margin under PSNR and SSIM respectively, partly because we rely entirely on SMPL to model the skeletal motion, while HumanNeRF optimizes the blend weights. And SelfRecon is based on surface rendering, which is less likely to generate noise compared to volume rendering. We believe that IntrinsicNGP can perform better with finer human surfaces. It should be noted that our method is only trained for about twenty minutes for each model on a single RTX3090, while the other methods need more than twelve hours.

Method	Dataset	PSNR $\uparrow$	SSIM $\uparrow$	Training time $\downarrow$
NeuralBody [22]	ZJU-Mocap	24.15	0.865	$\sim 12$ h
	Custom data	22.98	0.853	
AnimatableNeRF [21]	ZJU-Mocap	24.30	0.854	$\sim 12$ h
	Custom data	23.14	0.829	
HumanNeRF [31]	ZJU-Mocap	<b>25.99</b>	0.879	$\sim 12$ h
	Custom data	<b>26.38</b>	0.836	
SelfRecon [10]	ZJU-Mocap	25.20	<b>0.896</b>	$\sim 12$ h
	Custom data	25.16	<b>0.905</b>	
Ours	ZJU-Mocap	25.86	0.889	$\sim 20$ min
	Custom data	26.21	0.881	

Table 1. Quantitative comparison for novel view synthesis.

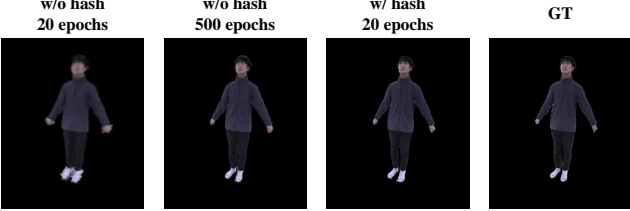


Figure 7. Ablation study on hash encoding.

### 4.3. Ablation Study

**Ablation Study on Multi-resolution Hash Encoding** To further verify the effectiveness of hash encoding in our method, we design the following baseline version. All the feature vectors originally obtained by hash encoding are now independent and optimizable. In practice, we directly anchor feature vectors on each corner of our UV-D grid. Then we use our custom data to train the original model and this pipeline. The corresponding rendering results are shown in Fig. 7. This representation takes at least ten times longer to converge. Using multi-resolution hash encoding dramatically increases the training speed of our method.

**Ablation Study on Offset Field** We attempt to remove the offset field (see Sec. 3.2) from our pipeline. As shown in Fig. 8, without the help of the offset field, our method generates blurry results. And the folds of the clothes turn to mean shapes without the offset field. The quantitative result in Tab. 2 illustrates that adding an offset field provides further gains. Therefore, we can see that the offset field can help model non-rigid deformation details.

**Ablation Study on UV-D Representation** To further evaluate the effectiveness of our intrinsic coordinate, we compare UV-D representation and XYZ-D representation defined in Sec. 3.2. Fig. 8 and Tab. 2 show the comparison result. Though XYZ-D representation can aggregate information across frames like UV-D representation, it is not easy to optimize an offset field based on XYZ-D representation. Therefore, the XYZ-D representation cannot handle clothing deformation and generates blurry results. As our UV-D grid is a smooth and convex domain, we can further refine the results within this domain.

	XYZ-D Representation	Without offset field	Full pipeline
PSNR	25.35	25.23	26.68
SSIM	0.889	0.887	0.913

Table 2. Quantitative result of ablation study on UV-D representation and offset field. We train these models on “Camera (1)” of “ZJU313” and use the remaining views for the test.

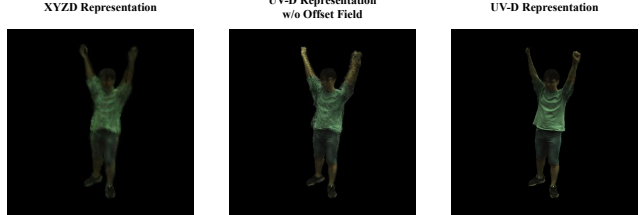


Figure 8. Ablation study on UV-D representation and offset field.

### 4.4. Application: Shape Editing

Since IntrinsicNGP’s representation is based on explicit human surfaces and our UV-D grid can be explained as a 3D density-color map. Therefore, the trained model can be used for shape editing by directly editing the input surfaces. Specifically, we edit the shape parameters of SMPL to generate new geometry proxies and render novel shape results with them. The qualitative results are shown in Fig. 6.

## 5. Limitation and Future Work

Currently, our method relies on the template model(in practical, SMPL). Although we employ the offset field to compensate for this, our approach is still limited by the expressiveness of the template model. Our proposed intrinsic coordinate-based INGP can not only be used for dynamic human performance but also can be easily extended to other dynamic objects with corresponding proxy geometry shapes for each frame, which may become our follow-up work.

## 6. Conclusion

We have proposed IntrinsicNGP, an effective and efficient novel view synthesis method for human performers based on the neural radiance field. We introduced a novel intrinsic coordinate representation, which could aggregate information across time and extend the hash encoding in INGP from static scenes to dynamic objects. For the captured human performer, IntrinsicNGP could converge to high-quality results within few minutes. Extensive experimental results have shown that we can generate high-fidelity results for this challenging task, demonstrating potential practical applications of IntrinsicNGP.

**Potential Negative Impact** Misuse of our method may raise ethical issues by reconstructing and generating a shape-edited human body without permission. Thus, we require that the media generated by our method clearly presents itself as synthetic.

**Acknowledgements** This work was supported by the National Natural Science Foundation of China (No. 62122071, No. 62272433).

## References

[1] Easymocap - make human motion capture easier. Github, 2021. [2](#), [3](#)

[2] Thiemo Alldieck, Marcus Magnor, Weipeng Xu, Christian Theobalt, and Gerard Pons-Moll. Video based reconstruction of 3d people models. In *Proceedings of the IEEE Conference on Computer Vision and Pattern Recognition*, pages 8387–8397, 2018. [1](#), [2](#), [3](#)

[3] Thiemo Alldieck, Mihai Zanfir, and Cristian Sminchisescu. Photorealistic monocular 3d reconstruction of humans wearing clothing. In *Proceedings of the IEEE/CVF Conference on Computer Vision and Pattern Recognition (CVPR)*, 2022. [3](#)

[4] Federica Bogo, Angjoo Kanazawa, Christoph Lassner, Peter Gehler, Javier Romero, and Michael J. Black. Keep it SMPL: Automatic estimation of 3D human pose and shape from a single image. In *Computer Vision – ECCV 2016*, Lecture Notes in Computer Science. Springer International Publishing, Oct. 2016. [1](#), [3](#)

[5] Ho Kei Cheng, Yu-Wing Tai, and Chi-Keung Tang. Modular interactive video object segmentation: Interaction-to-mask, propagation and difference-aware fusion. In *CVPR*, 2021. [3](#)

[6] Kangle Deng, Andrew Liu, Jun-Yan Zhu, and Deva Ramanan. Depth-supervised NeRF: Fewer views and faster training for free. In *Proceedings of the IEEE/CVF Conference on Computer Vision and Pattern Recognition (CVPR)*, June 2022. [3](#)

[7] Mingsong Dou, Sameh Khamis, Yury Degtyarev, Philip Davidson, Sean Ryan Fanello, Adarsh Kowdle, Sergio Orts Escolano, Christoph Rhemann, David Kim, Jonathan Taylor, et al. Fusion4d: Real-time performance capture of challenging scenes. *ACM Transactions on Graphics (ToG)*, 35(4):1–13, 2016. [1](#)

[8] Peter Hedman, Julien Philip, True Price, Jan-Michael Frahm, George Drettakis, and Gabriel Brostow. Deep blending for free-viewpoint image-based rendering. *ACM Transactions on Graphics (TOG)*, 37(6):1–15, 2018. [1](#)

[9] Yang Hong, Juyong Zhang, Boyi Jiang, Yudong Guo, Ligang Liu, and Hujun Bao. Stereopifu: Depth aware clothed human digitization via stereo vision. In *IEEE/CVF Conference on Computer Vision and Pattern Recognition (CVPR)*, pages 535–545, 2021. [3](#)

[10] Boyi Jiang, Yang Hong, Hujun Bao, and Juyong Zhang. Selfrecon: Self reconstruction your digital avatar from monocular video. In *IEEE/CVF Conference on Computer Vision and Pattern Recognition (CVPR)*, 2022. [3](#), [7](#), [8](#)

[11] Boyi Jiang, Juyong Zhang, Yang Hong, Jinhao Luo, Ligang Liu, and Hujun Bao. Bcnet: Learning body and cloth shape from a single image. In *European Conference on Computer Vision*. Springer, 2020. [3](#)

[12] Diederik P. Kingma and Jimmy Ba. Adam: A method for stochastic optimization. In Yoshua Bengio and Yann LeCun, editors, *3rd International Conference on Learning Representations, ICLR 2015, San Diego, CA, USA, May 7-9, 2015, Conference Track Proceedings*, 2015. [6](#)

[13] Nikos Kolotouros, Georgios Pavlakos, and Kostas Daniilidis. Convolutional mesh regression for single-image human shape reconstruction. In *Proceedings of the IEEE/CVF Conference on Computer Vision and Pattern Recognition*, pages 4501–4510, 2019. [1](#), [3](#)

[14] Youngjoong Kwon, Dahun Kim, Duygu Ceylan, and Henry Fuchs. Neural human performer: Learning generalizable radiance fields for human performance rendering. *Advances in Neural Information Processing Systems*, 34, 2021. [1](#), [2](#)

[15] Lingjie Liu, Marc Habermann, Viktor Rudnev, Kripasindhu Sarkar, Jiatao Gu, and Christian Theobalt. Neural actor: Neural free-view synthesis of human actors with pose control. *ACM Transactions on Graphics (TOG)*, 40(6):1–16, 2021. [1](#), [2](#)

[16] Stephen Lombardi, Tomas Simon, Jason Saragih, Gabriel Schwartz, Andreas Lehrmann, and Yaser Sheikh. Neural volumes: Learning dynamic renderable volumes from images. *ACM Trans. Graph.*, 38(4):65:1–65:14, July 2019. [3](#)

[17] Matthew Loper, Naureen Mahmood, Javier Romero, Gerard Pons-Moll, and Michael J. Black. SMPL: A skinned multi-person linear model. *ACM Trans. Graphics (Proc. SIGGRAPH Asia)*, 34(6):248:1–248:16, Oct. 2015. [3](#)

[18] Ben Mildenhall, Pratul P Srinivasan, Matthew Tancik, Jonathan T Barron, Ravi Ramamoorthi, and Ren Ng. Nerf: Representing scenes as neural radiance fields for view synthesis. In *European conference on computer vision*, pages 405–421. Springer, 2020. [1](#), [2](#), [3](#), [7](#)

[19] Thomas Müller. Tiny CUDA neural network framework, 2021. <https://github.com/hvlabs/tiny-cuda-nn>. [6](#)

[20] Thomas Müller, Alex Evans, Christoph Schied, and Alexander Keller. Instant neural graphics primitives with a multiresolution hash encoding. *ACM Trans. Graph.*, 41(4):102:1–102:15, July 2022. [1](#), [2](#), [3](#), [4](#), [5](#), [6](#)

[21] Sida Peng, Junting Dong, Qianqian Wang, Shangzhan Zhang, Qing Shuai, Xiaowei Zhou, and Hujun Bao. Animatable neural radiance fields for modeling dynamic human bodies. In *ICCV*, 2021. [1](#), [2](#), [7](#), [8](#)

[22] Sida Peng, Yuanqing Zhang, Yinghao Xu, Qianqian Wang, Qing Shuai, Hujun Bao, and Xiaowei Zhou. Neural body: Implicit neural representations with structured latent codes for novel view synthesis of dynamic humans. In *IEEE/CVF Conference on Computer Vision and Pattern Recognition (CVPR)*, pages 9054–9063, 2021. [1](#), [2](#), [7](#), [8](#)

[23] Christian Reiser, Songyou Peng, Yiyi Liao, and Andreas Geiger. Kilonerf: Speeding up neural radiance fields with thousands of tiny mlps. In *International Conference on Computer Vision (ICCV)*, 2021. [3](#)

[24] Shunsuke Saito, Zeng Huang, Ryota Natsume, Shigeo Morigi, Angjoo Kanazawa, and Hao Li. Pifu: Pixel-aligned implicit function for high-resolution clothed human digitization. In *IEEE/CVF International Conference on Computer Vision (ICCV)*, pages 2304–2314, 2019. [3](#)

[25] Sara Fridovich-Keil and Alex Yu, Matthew Tancik, Qinhong Chen, Benjamin Recht, and Angjoo Kanazawa. Plenoxels: Radiance fields without neural networks. In *CVPR*, 2022. [3](#)

[26] Shih-Yang Su, Frank Yu, Michael Zollhöfer, and Helge Rhodin. A-nerf: Articulated neural radiance fields for learning human shape, appearance, and pose. *Advances in Neural Information Processing Systems*, 34, 2021. [1](#), [2](#)

[27] Cheng Sun, Min Sun, and Hwann-Tzong Chen. Direct voxel grid optimization: Super-fast convergence for radiance fields reconstruction. In *CVPR*, 2022. [3](#)

[28] Jiaxiang Tang. Torch-ngp: a pytorch implementation of instant-ngp, 2022. <https://github.com/ashawkey/torch-ngp>. [6](#)

[29] Jiaxiang Tang, Xiaokang Chen, Jingbo Wang, and Gang Zeng. Compressible-composable nerf via rank-residual decomposition. *arXiv preprint arXiv:2205.14870*, 2022. [6](#)

[30] Matthias Teschner, Bruno Heidelberger, Matthias Müller, Danat Pomerantes, and Markus H Gross. Optimized spatial hashing for collision detection of deformable objects. In *Vmv*, volume 3, pages 47–54, 2003. [4](#)

[31] Chung-Yi Weng, Brian Curless, Pratul P. Srinivasan, Jonathan T. Barron, and Ira Kemelmacher-Shlizerman. HumanNeRF: Free-viewpoint rendering of moving people from monocular video. In *Proceedings of the IEEE/CVF Conference on Computer Vision and Pattern Recognition (CVPR)*, pages 16210–16220, June 2022. [1](#), [2](#), [7](#), [8](#)

[32] Liwen Wu, Jae Yong Lee, Anand Bhattad, Yu-Xiong Wang, and David Forsyth. Diver: Real-time and accurate neural radiance fields with deterministic integration for volume rendering. In *Proceedings of the IEEE/CVF Conference on Computer Vision and Pattern Recognition*, pages 16200–16209, 2022. [3](#)

[33] Yuliang Xiu, Jinlong Yang, Dimitrios Tzionas, and Michael J. Black. ICON: Implicit Clothed humans Obtained from Normals. In *Proceedings of the IEEE/CVF Conference on Computer Vision and Pattern Recognition (CVPR)*, pages 13296–13306, June 2022. [3](#)

[34] Hongyi Xu, Thieno Alldieck, and Cristian Sminchisescu. H-nerf: Neural radiance fields for rendering and temporal reconstruction of humans in motion. *Advances in Neural Information Processing Systems*, 34, 2021. [1](#), [2](#)

[35] Tianhan Xu, Yasuhiro Fujita, and Eiichi Matsumoto. Surface-aligned neural radiance fields for controllable 3d human synthesis. In *Proceedings of the IEEE/CVF Conference on Computer Vision and Pattern Recognition (CVPR)*, pages 15883–15892, June 2022. [2](#)

[36] Fuqiang Zhao, Wei Yang, Jiakai Zhang, Pei Lin, Yingliang Zhang, Jingyi Yu, and Lan Xu. Humannerf: Efficiently generated human radiance field from sparse inputs. In *Proceedings of the IEEE/CVF Conference on Computer Vision and Pattern Recognition (CVPR)*, pages 7743–7753, June 2022. [1](#), [2](#)